

# Comprehensive experimental test of quantum erasure

Alexei Trifonov,\* Gunnar Björk, Jonas Söderholm, and Tedros Tsegaye

Department of Electronics, Royal Institute of Technology (KTH), Electrum 229, SE-164 40 Kista, Sweden  
(February 1, 2008)

In an interferometer, path information and interference visibility are incompatible quantities. Complete determination of the path will exclude any possibility of interference, rendering the visibility zero. However, if the composite object and probe state is pure, it is, under certain conditions, possible to trade the path information for improved (conditioned) visibility. Such a procedure is called quantum erasure. We have performed such experiments with polarization entangled photon pairs. Using a partial polarizer we could vary the degree of entanglement between object and probe. We could also vary the interferometer splitting ratio and thereby vary the *a priori* path predictability. We have tested quantum erasure under a number of different experimental conditions and found good agreement between experiments and theory.

PACS numbers: 03.65.Bz, 42.50.-p

## I. INTRODUCTION

A fundamental difference between classical physics and quantum mechanics is that the latter, being a linear dynamical theory, allows superpositions. The superposition principle, in turn, leads directly to the concept of complementarity, the fact that any quantum system has at least two properties that cannot simultaneously be known. Complementarity [1,2] has been discussed intensively since the early development of quantum mechanics. Recently some new qualitative statements about complementarity have been proposed [3–12], and subsequently the question has been raised whether there exist any relations between these new expressions and the Schrödinger-Robertson and the Arthurs-Kelley uncertainty principles [8,9,11,13,14]. In addition, the fundamental physical mechanism that enforces complementarity has been debated [14–17]. The superposition principle also leads to nonlocality. This consequence of quantum theory led Einstein, Podolsky and Rosen to write their famous EPR-paper [18], arguing that this consequence of quantum theory rendered the theory “unreasonable”. Later Bell devised an experimental procedure in which predictions of quantum mechanics could be tested against predictions based on locally realistic theories [19]. Several such

experiments have been made [20–24] and all results have been compatible with the predictions of quantum mechanics.

When deriving his uncertainty principle, Heisenberg erroneously attributed the uncertainty to the back-action on the measured object from the measurement apparatus. Later work has clarified that Heisenberg’s uncertainty relation only makes a statement about the preparation of a quantum mechanical state. If one wants to qualitatively record the back-action on the state due to a measurement of some observable  $\hat{A}$ , one also has to measure the conjugate observable to  $\hat{A}$  on the “same” state. (Unless the state is an eigenstate of  $\hat{A}$  the state will change as a result of the  $\hat{A}$ -measurement, therefore we have put the word “same” in quotes.) This is often called a simultaneous measurement, i.e., on every state in an ensemble two incompatible measurements are made. To qualitatively describe the uncertainty product of the two simultaneous measurements one arrives at quantitatively or even qualitatively different uncertainty principles from that of Heisenberg [13,25–30]. What is surprising is that the back-action, or at least the measured uncertainty due to the back-action, is not solely a property of the object, and the object and probe interaction, but depends also on how the probe is measured and how the obtained information is used. Under certain circumstances, the apparent indeterminism of the object due to the measurement back-action can be undone by the action of a *local* operation on the probe. This procedure is called quantum erasing [31] and is a manifestation of the nonlocality of quantum mechanics. Various implementations of such experiments, and their connection to complementarity have been discussed in some recent papers [6,12,13,32]. Several experiments have also been performed [33–39]. What distinguishes our experiment from the previous ones is that we have been able to vary both the degree of object and probe entanglement and, independently, the *a priori* path information. This leads to a more complex situation than previously reported.

In order to discuss quantum erasure in greater detail we will start by making a few definitions. Quantum mechanics only makes predictions about states. It does not say anything about paths, modes or objects. All these words are classical concepts, but are nonetheless useful in discussions about quantum erasure. Usually quantum erasure is discussed in the context of an object taking one of two paths in an interferometer (or passing through one of two slits in a Young’s double-slit experiment). In a more strict manner of speaking the two paths are described by two orthogonal modes. The object, and its

---

\*Electronic address: alexei@ele.kth.se

Permanent address: Ioffe Physical Technical Institute, 26 Polytekhnicheskaya, 194021 St. Petersburg, Russia.

path is then defined by two state vectors  $|O_+\rangle$  and  $|O_-\rangle$ . In general this description is insufficient to describe all possible outcomes of an experiment. In this case it is more proper to define the object and its path by two sets of states  $\{|O_{+,i}\rangle\}$  and  $\{|O_{-,i}\rangle\}$ , where all states in one set are mutually orthonormal (and quite obviously all pairs of states from different sets are orthogonal). This is, e.g., the case in a recent experiment by Schwindt *et al.* [40], where the paths were defined in terms of two spatial modes, and in each of the paths the object could be either in a vertically or in a horizontally polarized state (or in a superposition or mixture of the two polarization states). However, to describe our experiment we shall only need to consider a two-dimensional object Hilbert space  $\mathcal{H}_O$ . Note that in defining the object in terms of a pair of orthonormal states, the concept of “path” should not be taken literally. In our experiment the two modes corresponding to the “paths” are actually two orthogonal linear polarization modes, or equivalently, two orthogonal polarization states in the same spatial mode.

To determine the state of the object, and hence identify the “path”, we need only a two dimensional probe Hilbert space  $\mathcal{H}_M$ , spanned by the two orthonormal state vectors  $|M_+\rangle$  and  $|M_-\rangle$ . In order to make any statement about the object’s “path” through a measurement of the probe, the object and the probe need to be in an entangled state described by the density matrix  $\hat{\rho}$  belonging to the space  $\mathcal{H}_O \otimes \mathcal{H}_M$ . In our experiment the preparation of  $\hat{\rho}$  is accomplished by a combination of photon-pair generation in a frequency down-converting nonlinear crystal and a partial polarizer interacting with the object.

The only *a priori* information we have are known the probabilities  $w_+$  and  $w_- = 1 - w_+$  for the two events. (These are given by the object state preparation.) The Maximum Likelihood (ML) estimation strategy (which is one of many possible strategies) dictates that we should, for each and every event, guess that the object took the most likely “path”. The strategy will maximize the likelihood  $L$  of guessing correctly. The likelihood will be  $L = \text{Max}\{w_+, w_-\}$ , and from this relation it is evident that  $1/2 \leq L \leq 1$ . The likelihood can be renormalized to yield the predictability  $P$  [10,11], given by

$$P = 2L - 1. \quad (1)$$

It is clear that  $0 \leq P \leq 1$ , where  $P = 0$  corresponds to a random guess of which “path” the object took, and  $P = 1$  corresponds to absolute certainty about the “path”.

One can also compute the visibility when the two “path” probability amplitudes interfere. The visibility  $V$ , too, is a statistical measure which requires an ensemble of identically prepared systems to estimate. The classical definition of  $V$  is

$$V = \frac{I_{\max} - I_{\min}}{I_{\max} + I_{\min}}, \quad (2)$$

where  $I_{\max}$  and  $I_{\min}$  are the intensities of the interference fringe maxima and minima. For a single quanta we

can only talk about the probability  $p$  of the object being detected on a specific location on a screen, or exiting one of two interferometer ports. (Do not confuse this probability  $p$  with the predictability  $P$ .) The probability  $p$  will vary essentially sinusoidally with position on the screen, or with the interferometer arm-length difference. In this case the natural definition of  $V$  is

$$V = \frac{p_{\max} - p_{\min}}{p_{\max} + p_{\min}}. \quad (3)$$

It has been shown [11] that  $P$  and  $V$  for an object whose “path” is determined by one of two orthonormal states, satisfies the following inequality:

$$P^2 + V^2 \leq 1, \quad (4)$$

where the upper bound is saturated for any pure state. Note that if one wants to verify the inequality (4) experimentally, one needs two ensembles of identical states. On the first ensemble one makes a “path” measurement and on the second one makes a visibility measurement. Hence, on any one state only one (sharp) measurement is performed.

## II. PROBING THE “PATH”

In order to retrieve more information about the “path” of the object then what is given by *a priori* knowledge of “path” probabilities (1), it is possible to use an ancillary probe system. By using a correlated ancillary system one can simultaneously get “path” information (from the probe ancilla) and visibility information (from the object). In the case where the Hilbert space of the object is two-dimensional, the probe must possess at least two degrees of freedom. Hence, in the simplest case the total system belongs to a  $2 \times 2$  dimensional composite Hilbert space. The measurement of “path” information and/or visibility must be preceded by an interaction between the object and probe which entangles their degrees of freedom. Hence the simplest state after the interaction will be a four-mode state consisting of the object, whose “path” and visibility information of we wish to measure, and the probe, which will help us to get information about the object’s “path”. We assume that an interaction between the object and probe leaves the probabilities  $w_+$  and  $w_-$  invariant. This is not the most general entangling interaction possible, it defines the subset of entangling interactions of the quantum non-demolition (QND) kind [12].

A few different experimental situations can be distinguished:

1. The state after the interaction can be factorized in the two composite Hilbert spaces  $\mathcal{H}_O$  and  $\mathcal{H}_M$ . Then both systems can be treated independently. The state of the probe carries no information about the object and vice versa. This is a trivial and not particularly interesting situation.

2. The state is a perfectly entangled state so that the probe contains full “path” information of the object. Thus no interference between the object “path” probability amplitudes can take place. Our ability to predict which “path” the object took is perfect, while the visibility is zero. It is possible, however, to retrieve the object preinteraction “path” interference visibility by doing a conditioned measurement. To retrieve the visibility, it is necessary to give up the “path” information. Therefore the probe must be measured in such a way that the information encoded in the state of the probe is not revealed by the measurement, i.e., the probe must be measured in such a way that the corresponding observable is complementary to the observable that discloses the “path”. For a pure state it is thus possible to restore the visibility of the initial state (conditioned visibility) with subsequent loss of the “path” information.

3. The state is partially entangled. This is an intermediate case between the previous two. Only partial information about the “path” of the object can be extracted from the probe. That still leaves room for non-zero “path” visibility. This intermediate case is examined carefully in the paper.

The most general scheme of the measuring procedure is shown in Fig. 1. The object can take one of two “paths” and the probe is used to determine which “path” the object took. Before the interaction (plane A) the object and the probe are independent and the state is represented by a product of the corresponding density operators:

$$\hat{\rho} = \hat{\rho}_O \otimes \hat{\rho}_M, \quad (5)$$

where  $\hat{\rho}_O = |\Psi_O\rangle\langle\Psi_O|$  and  $|\Psi_O\rangle = \sqrt{w_+}|O_+\rangle + e^{i\phi}\sqrt{w_-}|O_-\rangle$ . This is not the most general density operator since it represents a pure state, but since only pure states saturate Eq. (4) we will concentrate on this case in this work. The role of the interaction is to entangle the object and the probe. We assume that the interaction affects only the probe’s degrees of freedom and works like a unitary transformation

$$\begin{aligned} \hat{U}|O_+\rangle|M\rangle &= |O_+\rangle|m_+\rangle, \\ \hat{U}|O_-\rangle|M\rangle &= |O_-\rangle|m_-\rangle, \end{aligned} \quad (6)$$

where  $|M\rangle$  is the initial probe state. The state after the interaction (plane B) becomes

$$|\Psi_e\rangle = \sqrt{w_+}|O_+\rangle|m_+\rangle + e^{i\phi}\sqrt{w_-}|O_-\rangle|m_-\rangle. \quad (7)$$

The corresponding density operator is denoted  $\hat{\rho}_e$ . As mentioned above, this is not the most general case of entanglement (the general case is discussed in [12]) but sufficient for our task. If  $\langle m_+|m_- \rangle = 0$  (perfect entanglement) then the “path” the object took can be extracted perfectly from a measurement of the probe. It is convenient to introduce

$$c = |\langle m_+|m_- \rangle| \quad (8)$$

as a measure of entanglement. Note that  $c$  depends both on the state  $\hat{\rho}_e$  and also, in general, on the choice of the object basis. However, since the object basis is fixed, (the “path” is defined in terms of the fixed states  $|O_+\rangle$  and  $|O_-\rangle$ ),  $c$  is an unambiguous measure of the entanglement. If there is no entanglement then  $|m_+\rangle = |m_-\rangle$ , which implies  $c = 1$ .

From an experimental point of view it is more convenient to deal with an orthogonal probe basis  $|M_+\rangle$  and  $|M_-\rangle$ . It is always possible to choose, for simplicity,  $\langle m_+|m_- \rangle = 0$ . In this new basis

$$\begin{aligned} |\Psi_e\rangle &= \sqrt{w_+}|O_+\rangle|M_+\rangle + e^{i\phi}c\sqrt{w_-}|O_-\rangle|M_+\rangle \\ &\quad + e^{i\phi}\sqrt{w_-(1-c^2)}|O_-\rangle|M_-\rangle. \end{aligned} \quad (9)$$

One of the simplest experimental realizations of this state is a superposition of two single-photon two-mode states. Unfortunately the strength of the state-of-the-art nonlinear interaction at single photon level is too weak in order to produce the state (9) from (5) by interaction of object and probe photons. It is tempting to try however to simulate the state (9) as a result of spontaneous parametric down conversion (SPDC). In the process of SPDC the pump photon is split into a pair of photons. In Sec. 4 we will show that under a specific condition the state (9) can be produced. But first let us introduce the quantities of interest for a quantitative discussion of “path” and visibility information.

### III. DISTINGUISHABILITY AND VISIBILITY

The complementary nature of the object before the interaction is fully described by  $P$  and  $V$ . The predictability can be computed from  $\hat{\rho}_e$  as:

$$\begin{aligned} P &\equiv |w_+ - w_-| \\ &= |\langle O_+|\text{Tr}_M\{\hat{\rho}_e\}|O_+\rangle - \langle O_-|\text{Tr}_M\{\hat{\rho}_e\}|O_-\rangle|, \end{aligned} \quad (10)$$

where the trace is taken over the probe Hilbert space. By our choice of interaction (QND-type of entanglement) the predictability remains invariant, but the post-interaction visibility will, in general be smaller than the preinteraction visibility. The visibility can also be computed from  $\hat{\rho}_e$

$$V = 2|\langle O_+|\text{Tr}_M\{\hat{\rho}_e\}|O_-\rangle|. \quad (11)$$

These expressions are consistent with Eqs. (1) and (3). Since the visibility is not a conserved quantity, we will denote the preinteraction visibility  $V_0$ . In general  $V \leq V_0$ , which can be attributed to random relative-phase shifts associated with the interaction process [17].

The measure of the post-interaction “path” information is the distinguishability which is given by

$$D = \text{Tr}_M\{|\langle O_+|\hat{\rho}_e|O_+\rangle - \langle O_-|\hat{\rho}_e|O_-\rangle|\}, \quad (12)$$

where  $\|a\|$  denotes the trace-class norm of  $\hat{a}$  (see for example [41]). Choosing the entanglement interaction in the way we did ensures that  $P \leq D$ . As it was shown by Englert [11], complementarity leads to the inequality

$$D^2 + V^2 \leq 1. \quad (13)$$

This expression has a clear physical explanation: It is possible to get more information about the “path” ( $D$ ) only on the expense of the conjugate observable, which is the relative-phase and is quantified by ( $V$ ) for the discussed case [13,17]. It means that  $D$  contains both the *a priori* “path” information as well as the additional information encoded in the state of the probe. It should be noted that the distinguishability denotes the maximum information about the “path” that can be extracted from the probe by a measuring apparatus. Obtaining the full information can be accomplished for example by optimal probe state projection on photodetectors by adjusting the unitary evolution  $\hat{U}_M$  preceding the photodetectors (see Fig. 1). For an arbitrary, in general non-optimal probe measurement basis, the quantitative measure of obtained “path” information is the so-called measured distinguishability [12] (the same quantity is called “knowledge” by Englert [40]). It can mathematically be expressed:

$$D_m = \left| \langle M_+ | \hat{U}_m (\langle O_+ | \hat{\rho}_e | O_+ \rangle - \langle O_- | \hat{\rho}_e | O_- \rangle) \hat{U}_m^\dagger | M_+ \rangle \right| + \left| \langle M_- | \hat{U}_m (\langle O_+ | \hat{\rho}_e | O_+ \rangle - \langle O_- | \hat{\rho}_e | O_- \rangle) \hat{U}_m^\dagger | M_- \rangle \right|. \quad (14)$$

The associated visibility, conditioned on the outcome of the probe measurement, can similarly be expressed:

$$V_c = 2 \left| \langle M_+ | \hat{U}_m \langle O_+ | \hat{\rho}_e | O_- \rangle \hat{U}_m^\dagger | M_+ \rangle \right| + 2 \left| \langle M_- | \hat{U}_m \langle O_+ | \hat{\rho}_e | O_- \rangle \hat{U}_m^\dagger | M_- \rangle \right|. \quad (15)$$

To interpret the equation above in terms of a concrete measurement procedure, the visibility data should be sorted in two sets depending on the outcome of the probe measurement. The conditioned visibility then is the probability weighted average of the two obtained visibilities. It can be seen directly from the form of (11) and (15) that  $V \leq V_c \leq V_0$ . The relations between all quantities for a pure state are summarized in Table I and by the inequalities (4) and (13).

As it was shown in [13] there exists a mutual symmetry between  $P$  and  $V_0$ . The symmetry implies that the visibility can be treated as predictability if the observables corresponding to the “path” measurement and the visibility measurement are exchanged. However, entanglement of the kind (6) breaks this symmetry: with the chosen entanglement it is feasible to get more information about the “path”  $D \geq P$  (see Table I) but at the expense of the visibility. In the “best” case (optimal quantum erasure) it is possible only to restore initial visibility. This follows from our choice of entanglement. We

optimized the interaction to use the probe to encode the “path” information and not the complementary observable, which is quantified by the visibility.

#### IV. EXPERIMENTAL TEST OF COMPLEMENTARITY

A pair of photons entangled in polarization was used to produce the initial state (9). The experimental setup is shown in Fig. 2. It is similar to that described in [42]. The main difference is the use of a pulsed pump source (a Ti:Sapphire laser emitting at 780 nm) incorporating frequency doubling to 390 nm. The length of the pump pulse was chosen to be 1 ps which is long enough to minimize the group velocity dispersion problem. The use of a pulsed source reduced substantially the random coincidence counts between signal photons and dark counts and between coincident dark counts. Thus no dark-count corrections were made in any of the data presented in this paper. A beta-barium borate (BBO) crystal with type I phase matching was used for frequency doubling and a type II BBO crystal was used for SPDC. Special care was taken to compensate for the BBO group velocity mismatch. Photodetection was accomplished by EG&G single photon detectors with around 60% quantum efficiency. Identical 10 nm bandpass filters were placed in front of each of the detectors to select degenerate photon pairs. Two polarizers were used to select linearly polarized photons. Polarization rotation was accomplished by two  $\lambda/2$  plates placed before the polarizers. A 94% fringe visibility in coincidence measurement was observed when one  $\lambda/2$ -plate was fixed at 22.5 deg with respect to the BBO principal axes (horizontal-vertical) and the other  $\lambda/2$ -plate was rotated.

##### A. A maximally entangled state

Let us start with the state, which was produced in the experiment by the BBO-crystal (followed by state postselection to eliminate the predominant  $|0, 0\rangle$ -state):

$$|\Psi^-\rangle = \frac{1}{\sqrt{2}} (|\uparrow, \rightarrow\rangle - |\rightarrow, \uparrow\rangle), \quad (16)$$

or in a more suitable notation

$$|\Psi^-\rangle = \frac{1}{\sqrt{2}} (|O_+, M_+\rangle - |O_-, M_-\rangle). \quad (17)$$

This state corresponds to the second of the experimental situations listed in Sec. 2. For such a state  $P = 0$ ,  $D = 1$ , and  $V = 0$ . The measured distinguishability  $D_m(\theta)$  and the conditioned visibility  $V_c(\theta)$  were measured with respect to the probe basis rotation angle  $\theta$ :

$$\begin{pmatrix} |M_+(\theta)\rangle \\ |M_-(\theta)\rangle \end{pmatrix} = \hat{U}_m^\dagger \begin{pmatrix} |M_+\rangle \\ |M_-\rangle \end{pmatrix} = \begin{pmatrix} \cos\theta & \sin\theta \\ -\sin\theta & \cos\theta \end{pmatrix} \begin{pmatrix} |M_+\rangle \\ |M_-\rangle \end{pmatrix}, \quad (18)$$

where the angle  $\theta$  refers to the rotation angle from the horizontal plane. If the rotated probe measurement basis is used, the state (17) is written:

$$|\Psi^-\rangle = \frac{1}{\sqrt{2}} \{ \cos\theta [|O_+, M_+(\theta)\rangle - |O_-, M_-(\theta)\rangle] - \sin\theta [|O_+, M_-(\theta)\rangle - |O_-, M_+(\theta)\rangle] \}. \quad (19)$$

After a calculation using Eqs. (14) and (15) one finds  $D_m(\theta) = |\cos\theta|$  and  $V_c(\theta) = |\sin\theta|$ . Results of the measurements are shown in Fig. 3. Remember that the visibility of this state is zero for any probe measurement basis rotation. The degradation of the conditioned visibility due to the non-perfect mode overlap was taken into account in plotting the solid lines. This was done by multiplying the theoretically predicted conditioned visibility  $V_c$  by 0.94 which was the maximum experimentally obtained visibility. (For the particular entanglement we chose, the distinguishability relies on energy and momentum conservation, whereas good visibility also requires good mode overlap. The aforementioned group velocity dispersion associated with short orthogonally polarized photon pulses prevented us from getting perfect visibility as can be seen in the figure. Hence, the measured  $D_M$  goes from very close to unity to zero, whereas  $V_c$  goes from zero but only reaches 0.94 at its maximum point.) The apparent error in the figure is larger than the measurement error of  $D_m$  and  $V_c$  since it is the squares of these quantities, rather than the quantities themselves, that are plotted. We beg the reader to keep this point in mind in the following.

### B. A partially entangled state

A partial polarizer was inserted in the object beam rotated at an angle  $\alpha$  with respect to the horizontal plane (see Fig. 4). The partial polarizer consisted of a stack of  $N$  glass plates held at the Brewster angle with respect to the stack rotation axis. The amplitude transmittivities of the partial polarizer were  $t_p \approx 1$  and  $t_s = t$ , where  $t$  was determined by the number of plates  $N$ . (The indices p and s refer to the linear polarization states with the respect of the partial polarizer.)

In order to calculate the state after the polarizer it is convenient to rotate both bases so that the  $|O_+\rangle$  state becomes parallel to the p-plane of the partial polarizer

$$|\Psi^-\rangle = \frac{1}{\sqrt{2}} (|O_+(\alpha), M_+(\alpha)\rangle - |O_-(\alpha), M_-(\alpha)\rangle). \quad (20)$$

Now it is easy to find the state after the partial polarizer:

$$|\Psi_e\rangle = \frac{1}{\sqrt{1+t^2}} (|O_+(\alpha), M_+(\alpha)\rangle - t |O_-(\alpha), M_-(\alpha)\rangle). \quad (21)$$

A backward rotation by  $-\alpha$  gives

$$|\Psi_e\rangle = a_1 |O_+, M_+\rangle - a_2 |O_-, M_-\rangle + a_3 (|O_+, M_-\rangle - |O_-, M_+\rangle), \quad (22)$$

where

$$a_1 = \frac{t + (1-t)\cos^2\alpha}{\sqrt{1+t^2}}, \quad (23)$$

$$a_2 = \frac{t + (1-t)\sin^2\alpha}{\sqrt{1+t^2}}, \quad (24)$$

and

$$a_3 = \frac{(1-t)\sin\alpha\cos\alpha}{\sqrt{1+t^2}}. \quad (25)$$

Now let us find the correlation coefficients with respect to the probe basis rotation. As  $\theta$  is the angle of the probe measurement basis rotation, the state can be written as

$$|\Psi_e\rangle = b_1 |O_+, M_+\rangle - b_2 |O_-, M_-\rangle + b_3 |O_+, M_-\rangle + b_4 |O_-, M_+\rangle, \quad (26)$$

where  $b_1 = a_1 \cos\theta - a_3 \sin\theta$ ,  $b_2 = a_2 \cos\theta + a_3 \sin\theta$ ,  $b_3 = a_3 \cos\theta + a_1 \sin\theta$ , and  $b_4 = a_3 \sin\theta + a_2 \cos\theta$ . The photocount coincidence probabilities become

$$P_{++} = |\langle O_+, M_+(\theta) | \Psi_e \rangle|^2 = |b_1(\theta)|^2, \quad (27)$$

$$P_{--} = |\langle O_-, M_-(\theta) | \Psi_e \rangle|^2 = |b_2(\theta)|^2, \quad (28)$$

$$P_{+-} = |\langle O_+, M_-(\theta) | \Psi_e \rangle|^2 = |b_3(\theta)|^2, \quad (29)$$

and

$$P_{-+} = |\langle O_-, M_+(\theta) | \Psi_e \rangle|^2 = |b_4(\theta)|^2. \quad (30)$$

If we denote  $\theta_0$  to be the probe measurement angle defined by  $b_3(\theta_0) = 0$ , (for a pure state such an angle always exists) the relation between (9) and (26) is given as

$$w_+ = |b_1(\theta)|^2 + |b_3(\theta)|^2 = |b_1(\theta_0)|^2, \quad (31)$$

and

$$c = \sqrt{\frac{|b_4(\theta_0)|^2}{|b_2(\theta_0)|^2 + |b_4(\theta_0)|^2}} = \sqrt{\frac{|b_4(\theta_0)|^2}{1 - |b_1(\theta_0)|^2}}. \quad (32)$$

Knowing the correlation probabilities it is possible to derive quantities associated with the “path”:

$$\begin{aligned} P &= |w_+ - w_-| \\ &= ||b_1(\theta)|^2 + |b_4(\theta)|^2 - |b_2(\theta)|^2 - |b_3(\theta)|^2|, \end{aligned} \quad (33)$$

$$D_m(\theta) = ||b_1(\theta)|^2 - |b_3(\theta)|^2| + ||b_4(\theta)|^2 - |b_2(\theta)|^2|. \quad (34)$$

Conditioned visibility can be measured in the same way if we change the object detector basis from 0/90 deg to 45/135 deg. In the new basis the coincidence probabilities are

$$P_{45++} = \frac{|b_1(\theta) + b_4(\theta)|^2}{2}, \quad (35)$$

$$P_{45--} = \frac{|b_2(\theta) + b_3(\theta)|^2}{2}, \quad (36)$$

$$P_{45+-} = \frac{|b_3(\theta) - b_2(\theta)|^2}{2}, \quad (37)$$

$$P_{45-+} = \frac{|b_4(\theta) - b_1(\theta)|^2}{2}, \quad (38)$$

which makes it possible to calculate the quantities associated with relative phase measurements

$$V = |P_{45++}(\theta) - P_{45-+}(\theta) + P_{45+-}(\theta) - P_{45--}(\theta)|, \quad (39)$$

$$V_c(\theta) = |P_{45++}(\theta) - P_{45-+}(\theta)| + |P_{45+-}(\theta) - P_{45--}(\theta)|. \quad (40)$$

We measured the distinguishability and the conditioned visibility using eight different combinations of partial polarizer rotation angles and number of plates. Here we present only two of the combinations, but all the measurements were in good agreement with the theory.

### 1. Low a priori “path” information

The measured and calculated data for a home made, 10 plate, partial polarizer rotated by 43 degrees with respect to the horizontal plane are shown in Fig. 5. The 10 plate partial polarizer corresponds to  $t = 0.200$ . Using Eqs. (22), (8), (10), (11), and (12), we can compute the relevant parameters of the state to be  $c = 0.716$ ,  $P = 0.065$ ,  $V = 0.925$ , and  $D = 0.381$ , while a direct measurement gives  $P = 0.070$ ,  $V = 0.940$ , and  $D = 0.367$ , via Eqs. (33), (34), and (39). ( $D$  is the maximum of  $D_m(\theta)$  while  $V$  is the minimum of  $V_c(\theta)$ .) The state differs from the previous one in that although the predictability is almost zero, the distinguishability is nowhere near unity. That is, the object and the probe are only weakly entangled. The results for the  $D_m$  and  $V_c$  measurements are shown in Fig. 6. One should note specifically that as predicted  $D_m$  is bound from below by  $P$ , and from above by  $D$ . In the same manner we see that  $V_c$  is bound from below by  $V$ , and from above by  $(1 - P^2)^{1/2}$ .

It should be noted that the primary data, Fig. 5, agrees better with theory than the secondary data, Fig. 6. We suspect that the origin of this effect can be traced to our home made partial polarizer. The partial polarizer glass plates were not mounted perfectly in parallel. In an independent measurement we recorded the transmission of the polarized laser light (before the frequency doubling) through the partial polarizer as a function of the rotation angle  $\alpha$ . The transmission curves should be a displaced cosine curve which was not quite the case for our polarizer. However, since we did not possess a goniometer

it was hard to confirm that the suspected imperfection was indeed the cause, so we have opted to publish the uncorrected data.

We can also note that when the state is not perfectly entangled,  $D_m^2 + V_c^2$  is not a conserved quantity although the state is pure, confirming the predictions in [12]. The reason is that the observable corresponding to  $V_c$  in this case is not strictly complementary to the observable corresponding to  $D_m$ . Therefore the distinguishability measurement and the visibility measurement does not strictly probe complementary information about the state. However, the sum  $D_m^2 + V_c^2$  saturates the bound (13) when  $D_m = D$ , in accordance with the predictions of [12]. The sharp “corners” in the theoretical curves signify those rotation angles where the maximum likelihood strategy dictates a change in how the probe measurement outcomes should be used for the “path” estimation.

### 2. High a priori “path” information

The next example of a complementarity measurement is shown in Fig. 7 and Fig. 8. In this measurement a seven plate glass stack was used as a partial polarizer and the angle of rotation was adjusted to 21 deg. This corresponds to amplitude transmittivity  $t = 0.324$ . From these data we can calculate that  $c = 0.828$ ,  $P = 0.643$ ,  $V = 0.563$ , and  $D = 0.839$ , which are close to the values from the experimental values  $P = 0.639$ ,  $V = 0.550$ , and  $D = 0.839$ . This state is characterized by its large predictability, in contrast to the previously treated states. Since  $D$  must be larger than or equal to  $P$ , it also means that the distinguishability is high.

In Fig. 8 an even stranger shape of the function  $D_m^2 + V_c^2$  is seen. Since the predictability is large, there is little information to be had from the probe. We see that for most probe measurement bases the measured distinguishability cannot be improved beyond the *a priori* predictability. Only within a small interval of probe measurement rotations will the information encoded in the state of the probe improve the measured distinguishability, rendering it (at best) equal to  $D$ . Similarly, for most rotations the conditioned visibility does not exceed the visibility  $V$ . For the meter basis rotations between about 10 and 30 degrees (in theory) or between 10 and 20 degrees (in the experiment), both the measured distinguishability and the conditioned visibility attain their respective minimum values simultaneously. Here, the state is prepared in such a way that the “proper” complementary observable (as defined in [13]) is complementary both to the “path” observable and the conditioned visibility observable. This is a manifestation of the fact that any Hilbert space of dimension 2 allows three mutually complementary observables.

## V. CONCLUSIONS

The complementarity relation quantitatively derived by Englert [11] between “path” information and “path” interference visibility was tested under a wide range of experimental situations. Using a partial polarizer we were able to generate states with different *a priori* “path” information and different degrees of entanglement. The experiment was designed to, as close as possible, be an implementation of the theory in [11] and [12]. This is in contrast to a recent experiment by Schwindt *et al.* [40], where complementarity is tested without employing entanglement and with a larger object Hilbert space than the two dimensional space prescribed by the theory in [11]. The latter experiment can be analyzed and fully understood in terms of classical physics, whereas the experiment above, and, e.g., the experiments reported in [34–37] employ entangled states and hence quantum non-locality. By changing the measurement basis of the probe (a local operation) and by using conditioned measurements, the experiments gave us the possibility to verify the complementarity relations encompassing quantum erasure [12]. For non-ideal ( $P \geq 0$ ,  $D \leq 1$ ) but pure composite states, such a test yields rather surprisingly, only piecewise differentiable curves, reflecting the nonlinear maximum likelihood estimation strategy underlying the theory. The experimental results were in good agreement with theoretical predictions.

## ACKNOWLEDGMENTS

This work was supported by grants from the Swedish Technical Science Research Council, the Swedish Natural Science Research Council, the Royal Swedish Academy of Sciences, and by INTAS through Grant 167/96.

- 
- [1] W. Heisenberg, Z. Phys. **43**, 172 (1927); H. P. Robertson, Phys. Rev. **35**, 667A (1930); **46**, 7941 (1934); E. Schrödinger, Proc. Prussian Acad. Sci. Phys. Math. Sec. **XIX**, 296 (1930).
  - [2] N. Bohr, Nature **121**, 580 (1928).
  - [3] W. K. Wootters and W. H. Zurek, Phys. Rev. D **19**, 473 (1979).
  - [4] D. M. Greenberger and A. Yasin, Phys. Lett. A **128**, 391 (1988).
  - [5] L. Mandel, Opt. Lett. **16**, 1882 (1991).
  - [6] M. O. Scully, B.-G. Englert, and H. Walther, Nature (London) **351**, 111 (1991).
  - [7] M. G. Raymer and S. Yang, J. Mod. Opt. **39**, 1221 (1992).
  - [8] R. Bhandari, Phys. Rev. Lett. **69**, 3720 (1992).
  - [9] S. M. Tan and D. F. Walls, Phys. Rev. A **47**, 4663 (1993).
  - [10] G. Jaeger, A. Shimony, and L. Vaidman, Phys. Rev. A **51**, 54 (1995).
  - [11] B. G. Englert, Phys. Rev. Lett. **77**, 2154 (1996).
  - [12] G. Björk and A. Karlsson, Phys. Rev. A **58**, 3477 (1998).
  - [13] G. Björk *et al.*, Phys. Rev. A **60**, 1874 (1999).
  - [14] E. P. Storey, S. M. Tan, M. J. Collet, and D. F. Walls, Nature (London) **367**, 626 (1994).
  - [15] B.-G. Englert, M. O. Scully, and H. Walther, Nature (London), **375**, 367 (1995); E. P. Storey, S. M. Tan, M. J. Collet, and D. F. Walls, *ibid.* **375**, 368 (1995).
  - [16] H. M. Wiseman and F. E. Harrison, Nature (London) **377**, 584 (1995); H. M. Wiseman *et al.*, Phys. Rev. A **56**, 55 (1997).
  - [17] A. Luis and L. L. Sánchez-Soto, Phys. Rev. Lett. **81**, 4031 (1998).
  - [18] A. Einstein, B. Podolsky, and N. Rosen, Phys. Rev. **47**, 777 (1935).
  - [19] J. S. Bell, Rev. Mod. Phys. **38**, 447 (1966); Physics **1**, 195 (1964).
  - [20] A. Aspect, P. Grangier, and G. Roger, Phys. Rev. Lett. **49**, 91 (1982).
  - [21] T. E. Kiess, Y. H. Shih, A. V. Sergienko, and C. O. Alley, Phys. Rev. Lett. **71**, 3893 (1993).
  - [22] P. R. Tapster, J. G. Rarity, and P. C. M. Owens, Phys. Rev. Lett. **73**, 1923 (1994).
  - [23] E. S. Fry, T. Walther, and S. Li, Phys. Rev. A **52**, 4381 (1995).
  - [24] G. Weihs *et al.*, Phys. Rev. Lett. **81**, 5039 (1998).
  - [25] E. Arthurs and J. L. Kelly Jr., Bell Syst. Tech. J. **44**, 725 (1965).
  - [26] E. Arthurs and M. S. Goodman, Phys. Rev. Lett. **60**, 2447 (1988).
  - [27] C. Y. She and H. Heffner, Phys. Rev. **152**, 1103 (1966).
  - [28] S. Stenholm, Ann. Phys. (N.Y.) **218**, 233 (1992).
  - [29] H. Martens and W. M. de Muynck, J. Phys. A: Math. Gen. **25**, 4887 (1992).
  - [30] D. M. Appleby, Int. J. Theor. Phys. **37**, 1491 (1998); J. Phys. A **31**, 6419 (1998).
  - [31] M. O. Scully and K. Drühl, Phys. Rev. A **25**, 2208 (1982).
  - [32] P. G. Kwiat, A. M. Steinberg, and R. Chiao, Phys. Rev. A **49**, 61 (1994).
  - [33] P. G. Kwiat, A. M. Steinberg, and R. Chiao, Phys. Rev. A **45**, 7729 (1992).
  - [34] T. J. Herzog, P. G. Kwiat, H. Weinfurter, and A. Zeilinger, Phys. Rev. Lett. **75**, 3034 (1995).
  - [35] T. B. Pittman *et al.*, Phys. Rev. Lett. **77**, 1917 (1996).
  - [36] S. Dürr, T. Nonn, and G. Rempe, Phys. Rev. Lett. **81**, 5705 (1998).
  - [37] Y.-H. Kim, R. Yu, S. P. Kulik, Y. H. Shih, and M. O. Scully, Los Alamos e-print archive quant-ph/9903047.
  - [38] Z. Y. Ou *et al.*, Phys. Rev. A **41**, 566 (1990); Z. Y. Ou, Phys. Lett. A **226**, 323 (1997).
  - [39] X. Y. Zou, L. J. Wang, and L. Mandel, Phys. Rev. Lett. **67**, 318 (1991); A. G. Zajonc, L. J. Wang, X. Y. Zou, and L. Mandel, Nature (London) **353**, 597 (1991).
  - [40] P. D. D. Schwindt, P. G. Kwiat, and B.-G. Englert, Phys. Rev. A **60**, 4285 (1999).
  - [41] J. R. Klauder and E. C. G. Sudarshan, *Fundamentals of quantum optics* (Benjamin, New York, 1968).
  - [42] P. G. Kwiat *et al.*, Phys. Rev. Lett. **75**, 4337 (1995).

## VI. CAPTIONS

FIG. 1. Schematic setup for a QND-type measurement of the complementary “path” and visibility observables.  $\hat{U}_m$  symbolizes a local probe unitary transformation before probe state is irrevokably collapsed by the “which-path” meter.

FIG. 2. Experimental setup for testing complementarity by the means of photon polarization measurements on maximally entangled photon pairs. The labels SPC, P and  $\lambda/2$  signify single photon counters, polarizers and half-wave plates, respectively.

FIG. 3. Results for measured distinguishability and conditioned visibility versus probe meter basis rotation. Lines represent a theoretical simulation.

FIG. 4. Experimental setup for non-perfect QND-type measurements of photon polarization.

FIG. 5. Coincidence probabilities versus probe meter basis rotation after a 10 plate partial polarizer, rotated by  $\alpha = 43$  degrees with respect to the horizontal plane, was inserted in the object beam.

FIG. 6. Results for measured distinguishability and conditioned visibility versus meter basis rotation for the case of low *a priori* “path” information.

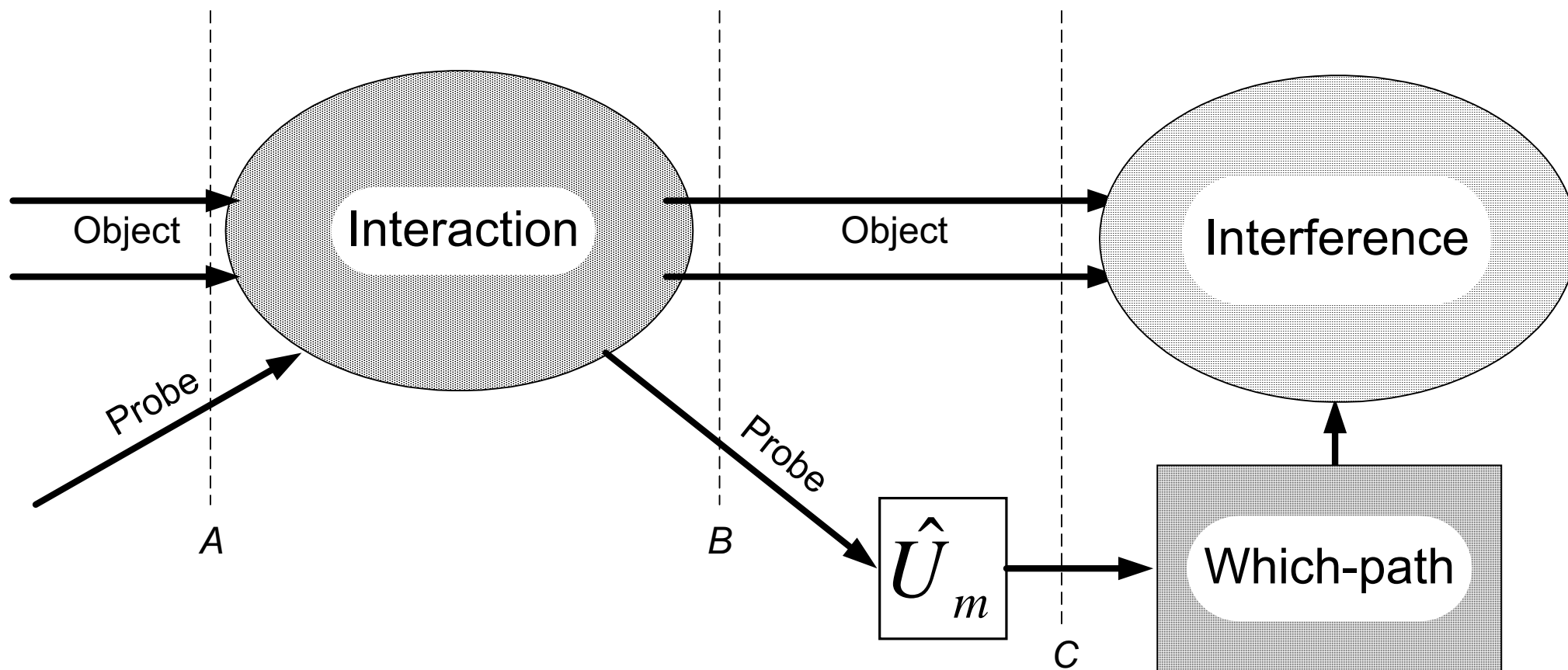
FIG. 7. Coincidence probabilities versus meter basis rotation after a 7 plate partial polarizer, rotated by  $\alpha = 21$  degrees with respect to the horizontal plane, was inserted in the object beam.

FIG. 8. Results for measured distinguishability and conditioned visibility versus probe meter basis rotation for the case of high *a priori* “path” information.

TABLE I. Which-path and visibility quantities, and their mutual relations.

	Quantities determined by the reduced object state $\hat{\rho}_O = \text{Tr}_M\{\hat{\rho}\}$		Quantities determined by the composite state $\hat{\rho}$ and the choice of probe basis		Quantities determined by the composite state $\hat{\rho}$
“Which path”	$P$	$\leq$	$D_m$	$\leq$	D
Visibility	$V = \sqrt{1 - D^2}$	$\leq$	$V_c$	$\leq$	$V_0 = \sqrt{1 - P^2}$





*Fig. 1. Trifonov et al Comprehensive test of the quantum erasure*

# BBO Type II

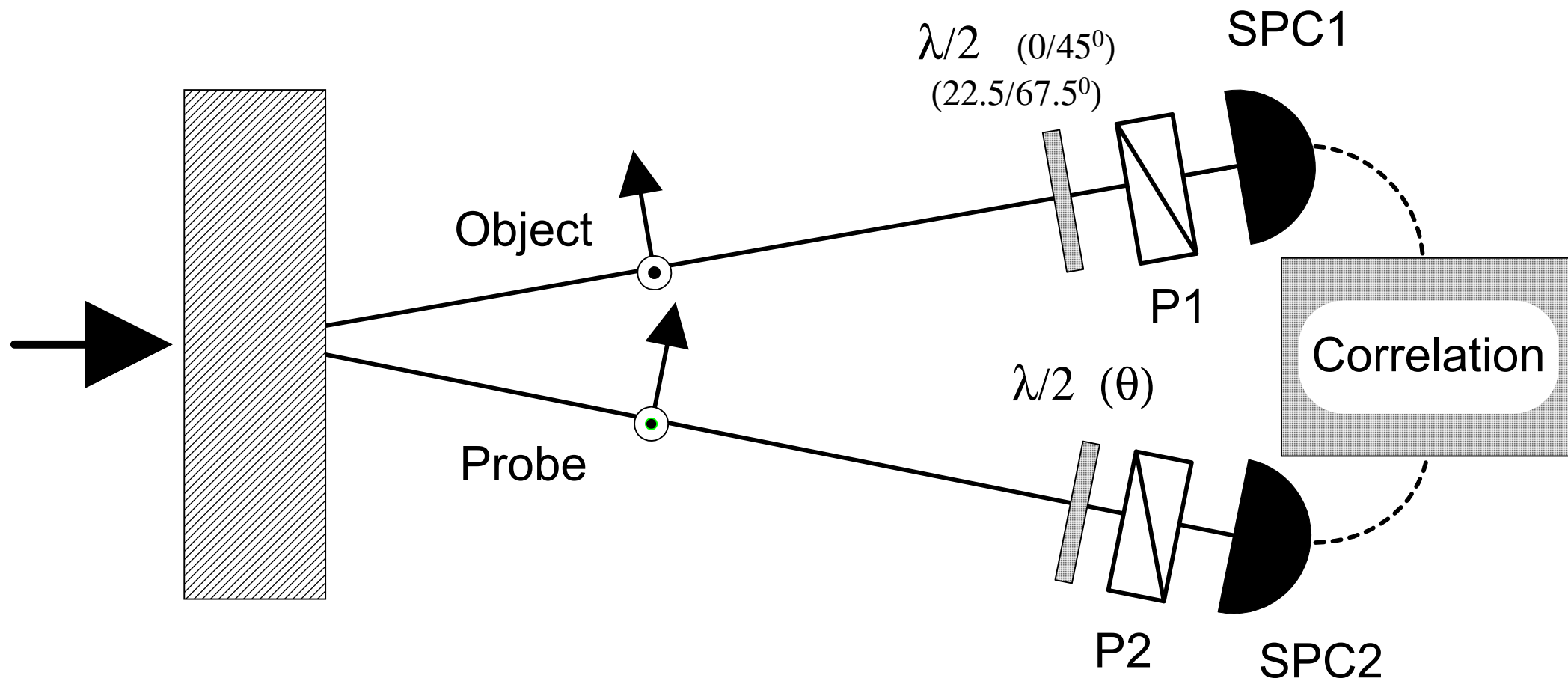


Fig. 2. Trifonov et al

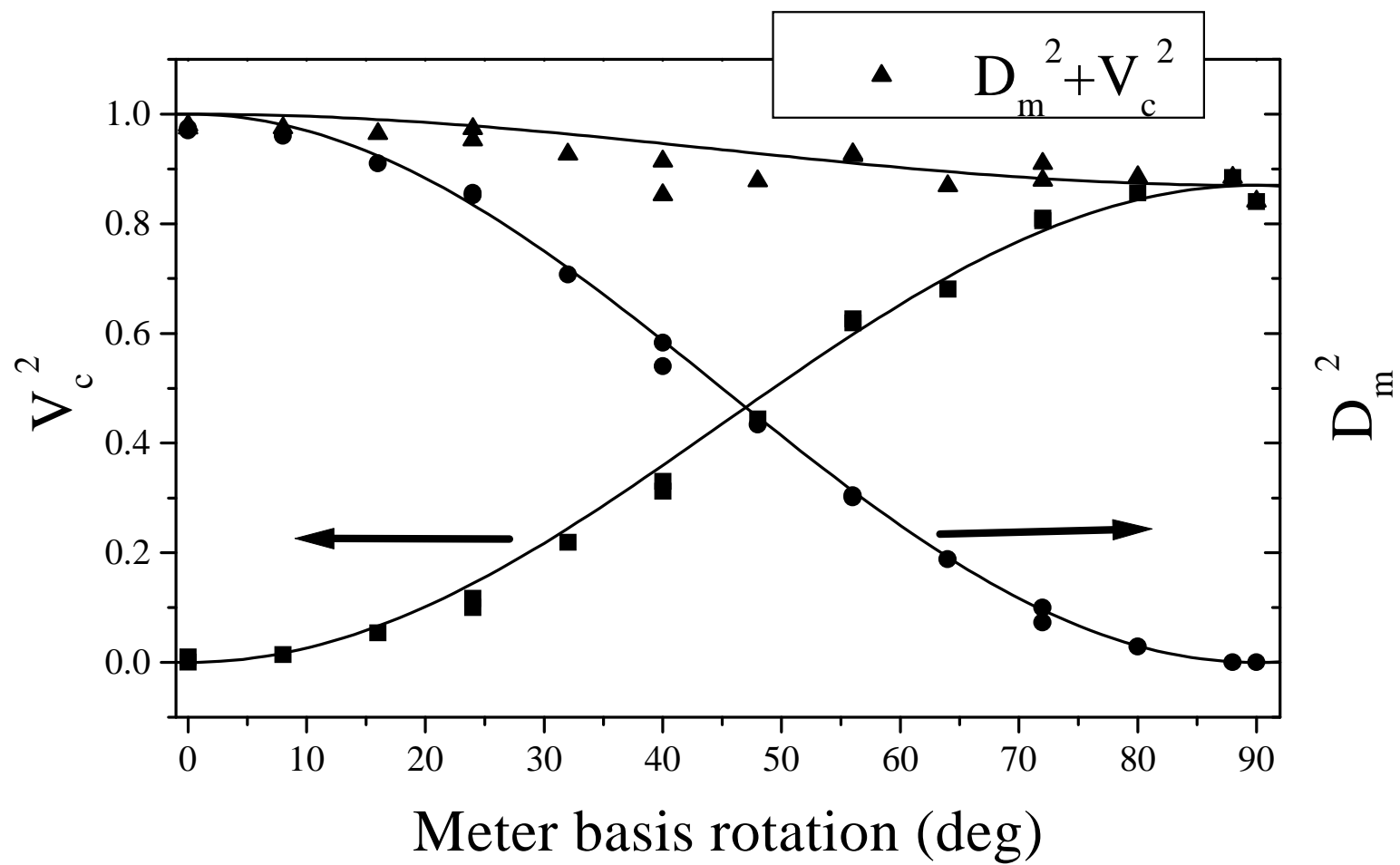
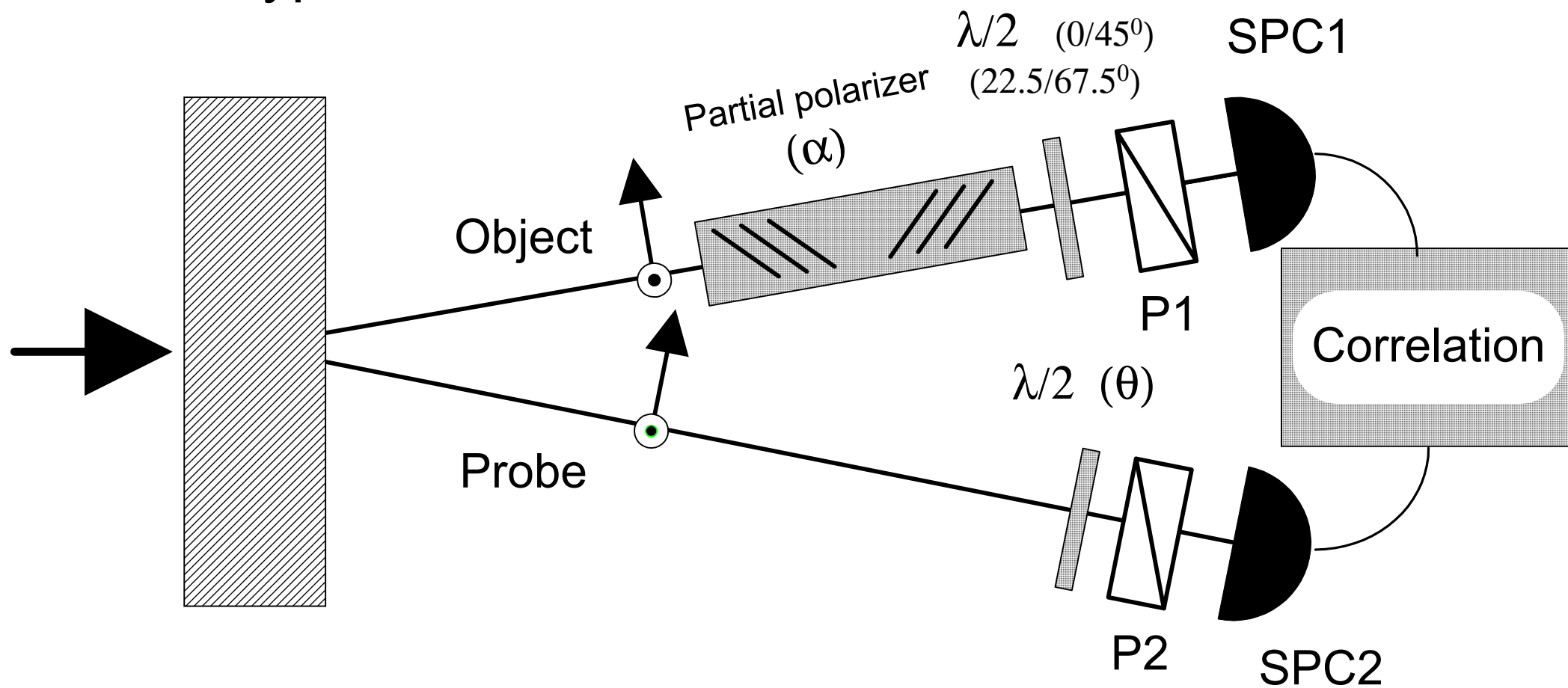
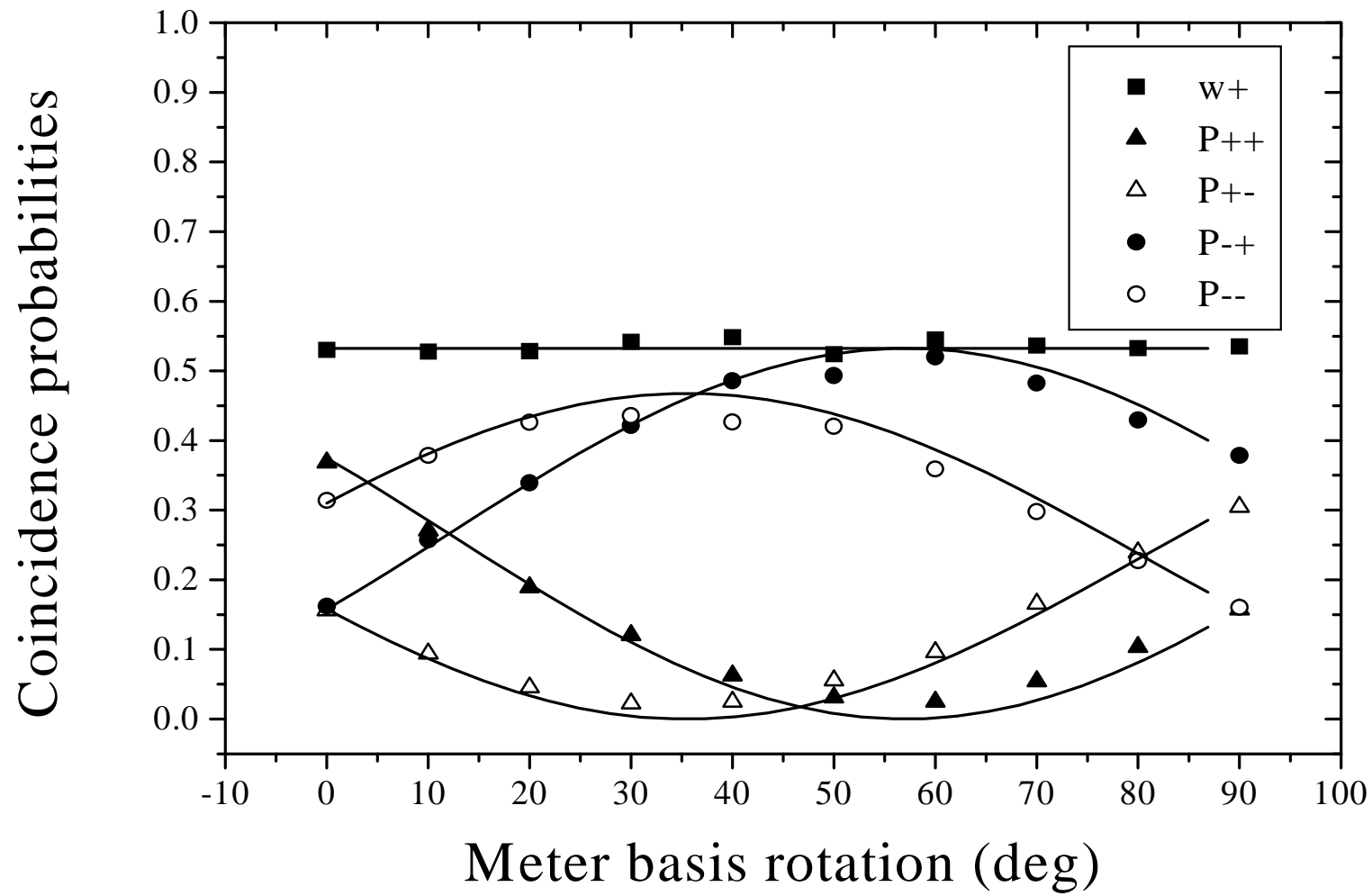


Fig.3 Trifonov et al

# BBO Type II



*Fig.4 Trifonov et al*



*Fig.5 Trifonov et al*

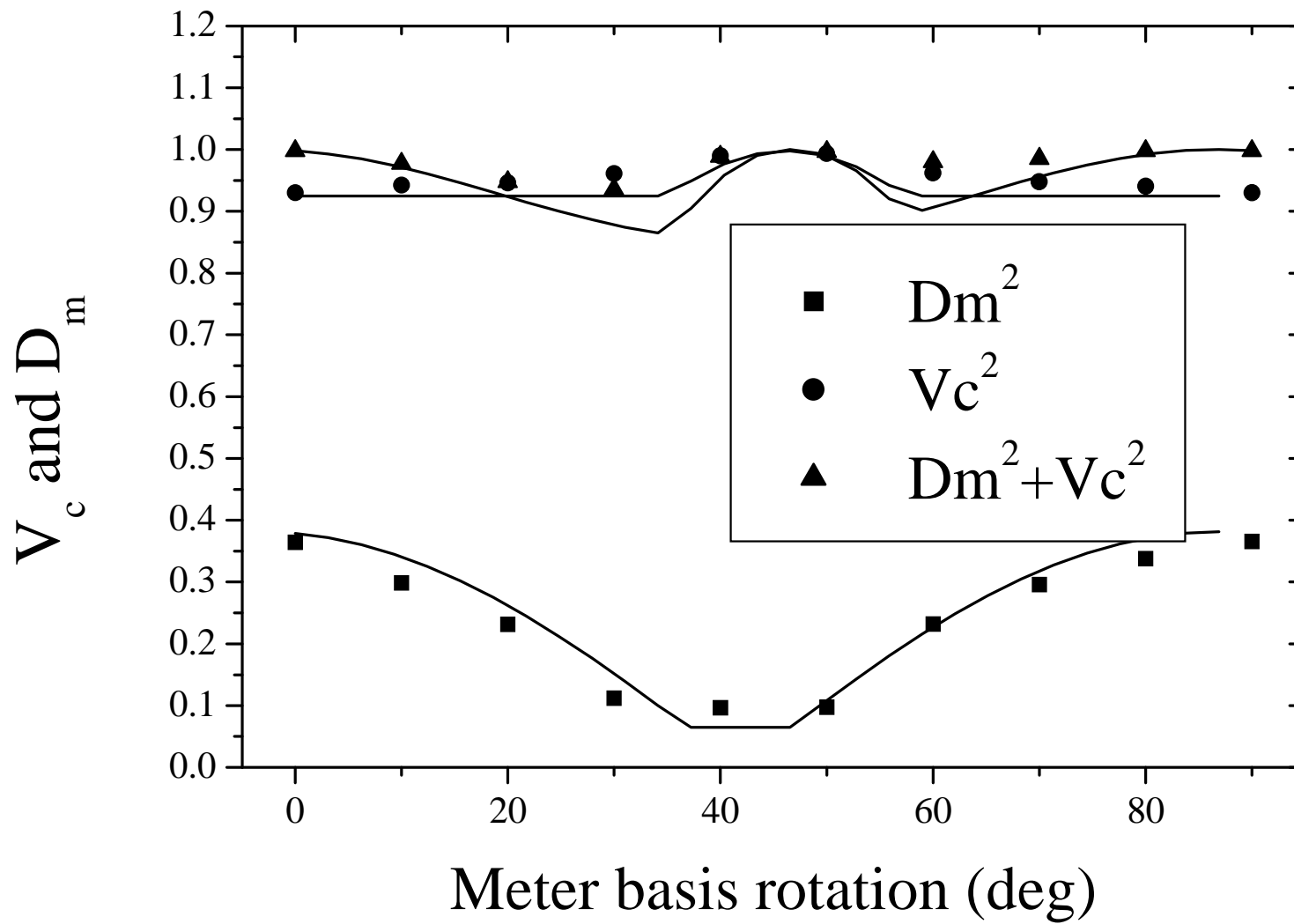
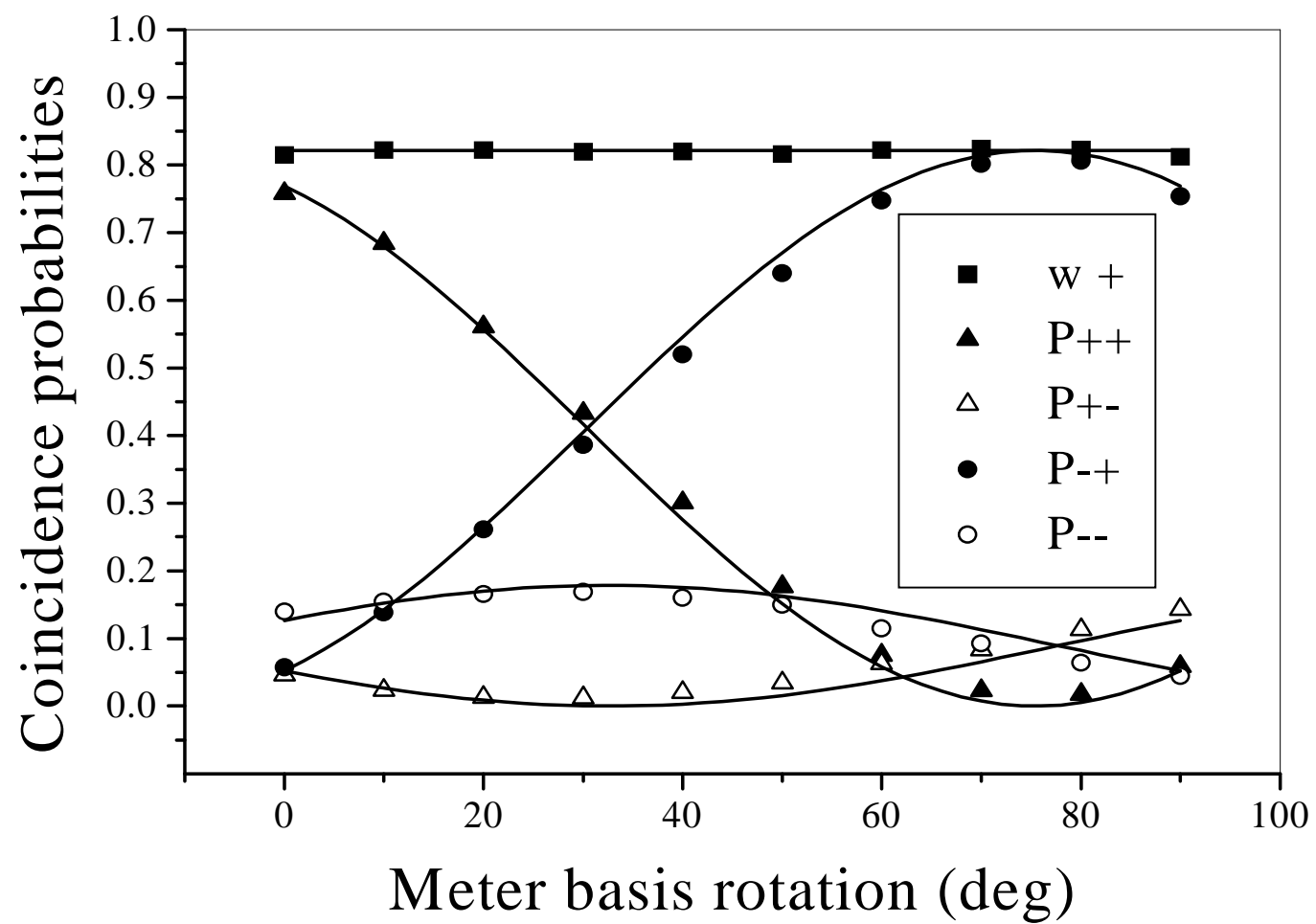
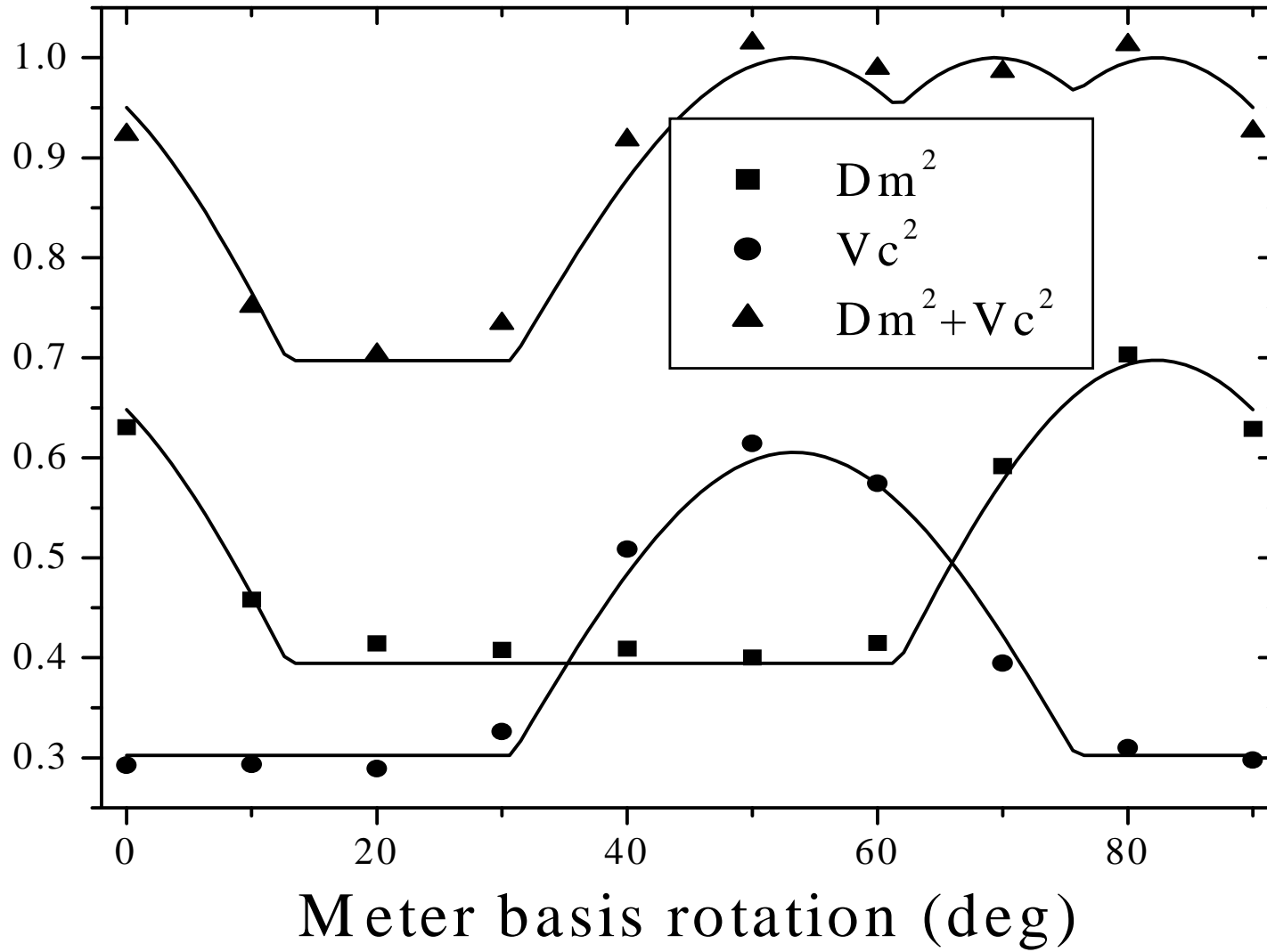


Fig.6 Trifonov et al



*Fig.7 Trifonov et al*



*Fig. 8 Trifonov et al*